# An Improved Current Error Control Strategy for Suppressing Subsequent Commutation Failures

2025 10th International Conference on Power and Renewable Energy (ICPRE) | 979-8-3315-8662-1/25/$31.00 ©2025 IEEE | DOI: 10.1109/ICPRE67300.2025.11274213

Chongru Liu
*School of Electrical and Electronic Engineering*
*North China Electric Power University*
Beijing, China
chongru.liu@ncepu.edu.cn

Haoyun Dong
*School of Electrical and Electronic Engineering*
*North China Electric Power University*
Beijing, China
haoyun.dong@ncepu.edu.cn

Yipeng Lv
*School of Electrical and Electronic Engineering*
*North China Electric Power University*
Beijing, China
lvyipeng2000@ncepu.edu.cn

Peinan Wang
*School of Electrical and Electronic Engineering*
*North China Electric Power University*
Beijing, China
3522476394@qq.com

Zhixian Li
*Power Dispatch Control Center*
*State Grid Zhengzhou Electric Power Co., LTD*
*Zhengzhou, China*
lizhixian777@163.com

Chenbo Su*
*School of Electrical and Electronic Engineering*
*North China Electric Power University*
*Beijing, China*
scb2636@foxmail.com
*Corresponding author

Jiashu Fang
*School of Mechanical and Electrical Engineering*
*University of Electronic Science and Technology of China*
Chengdu, China
jiashu.fang@hotmail.com
*Corresponding author

***Abstract*—Current Error Control (CEC) is vital for suppressing subsequent commutation failures (SCF) in Line-Commutated Converter High Voltage Direct Current (LCC-HVDC) systems. However, conventional CEC strategies, relying solely on commutation voltage, suffer from over-/under-compensation and inadequate SCF suppression during asymmetrical faults. This paper proposes a novel CEC strategy to address these limitations. Firstly, a commutation capability index ($S_{CCI}$) is defined based on Critical Commutation Area Theory (CCAT). Secondly, leveraging $S_{CCI}$, a dynamic CEC slope calculation method is proposed to eliminate over-/under-compensation. Finally, simulation studies on the CIGRE benchmark HVDC model within PSCAD/EMTDC validate the effectiveness of the proposed strategy in significantly enhancing SCF suppression.**

***Keywords—HVDC, subsequent commutation failure, commutation capability index, current error controller***

## I. Introduction

With the rapid growth of power loads and renewable energies, Line-Commuted Converter High Voltage Direct Current (LCC-HVDC) has become prevalent in modern power grids for long-distance power transmission [1]-[3]. Nevertheless, due to the lack of self-turn-off ability, thyristors based LCC-HVDC systems usually suffer from commutation failure, adversely affecting the safe operation of the power system [4]-[6]. Specifically, improper interactions of the controllers in LCC-HVDC would induce subsequent commutation failures (SCF) during the recovery process, potentially causing DC blocking and interrupting power transmission [7]. Hence, it is necessary to investigate strategies that can effectively suppress SCF [8].

For this purpose, some literature studied the mechanism and influencing factors of SCF. It is figured out in [9] that small variations in commutation voltage can lead to SCF when both the inverter and rectifier are in constant current control (CC) mode. In [10] and [11], the influence of the inverter bus's harmonic voltage and reactive power consumption on SCF are analyzed separately. Moreover, according to [12] and [13], the main factor leading to SCF is the uncontrolled decrease in the extinction angle when transitioning from CC to constant extinction angle control (CEA). Therefore, it is necessary to improve the coordination between CC and CEA controllers, taking into account the influencing factors of SCF.

It's worth noting that current error control (CEC) focuses on the control switch between the CC and CEA [14]. When the DC current is lower than the reference value, CEC can compensate for the extinction angle to accelerate the control switching from CC to CEA, thereby increasing the commutation margin [15]. From this perspective, improving CEC is an effective way to suppress SCF. A control strategy that dynamically adjusts the extinction angle increment through CEC is presented in [15], considering the severity of AC faults. Expanding on [15], the upper limit and the start voltage of CEC are further modified to enhance DC power transmission during fault [16]. An adaptive method is proposed for adjusting the slope of CEC based on changes in the system state [17]. A method to improve the coordination between controllers is proposed in [18], accelerating the control switching from CC to CEA.

However, researches about CEC still have some limitations for suppressing SCF. Firstly, in order to effectively suppress SCF, the index for evaluating the demand and capability of commutation is needed. Nevertheless, the existing indexes fail

This research is supported by the National Natural Science Foundation of China (U23B20126) and in part by the Science and Technology Project of State Grid Corporation of China (5100-202055476A-0-0-00).

to consider the fluctuations of the variations during the commutation process, thus leading to inaccurate evaluation [19]-[21]. Furthermore, the existing CEC strategies set parameters according to specific conditions rather than adaptively adjusting, which may impede the recovery process and further result in poor effectiveness on SCF suppression.

Addressing the existing research gaps, this work presents an improved CEC strategy for SCF suppression. Firstly, based on the critical commutation area theory (CCAT), an index ($S_{CCI}$) to evaluate the system commutation capability is proposed. Moreover, a dynamic calculation method for CEC slope is further proposed based on $S_{CCI}$. Finally, simulation experiments are tested to validate the effectiveness of the proposed strategy. The main contributions of this work can be summarized as follows:

1) To accurately evaluate the system's commutation capability, this paper introduces an index $S_{CCI}$, considering the fluctuations of variations during the commutation process.

2) To address the challenges of over-compensation and under-compensation, a dynamic CEC slope calculation method is proposed based on the proposed $S_{CCI}$. This method enables adaptive adjustment of the CEC output to meet the system's commutation requirements, effectively suppressing SCF.

3) The proposed strategy was tested under multiple operating conditions, demonstrating its effectiveness in suppressing SCF.

The remainder of this paper is organized as follows. Section II first introduces the critical commutation area theory, then defines the $S_{CCI}$ index to evaluate commutation capability. Section III first analyses the issue of over-compensation and under-compensation, then proposes a dynamic calculation method of CEC slope. Section IV conducts simulations to verify the effectiveness of the improved CEC control. Finally, Section V provides the conclusion of the paper.

## II. Commutation Capability Index

### *A. Critical Commutation Area Theory*

The critical commutation area theory CCAT establishes the energy equilibrium principle for commutation processes through energy demand and energy supply. Considering the commutation process from the 6-pulse bridge converter's valve VT1 to VT3 in Fig. 1, the commutation process follows:

$$L_C \frac{di_1(t)}{dt} - L_C \frac{di_3(t)}{dt} = \sqrt{2}U_{si} \sin \omega t \tag{1}$$

Where, $U_{si}$ represents the magnitude of the AC bus voltage on the inverter side, $\omega$ represents the system frequency.

The commutation process starts at $t_1=\alpha/\omega$, and ends at $t_2=(\alpha+\mu)/\omega=(\pi-\gamma)/\omega$ [22], where $\alpha$, $\mu$, and $\gamma$ represent the trigger angle, commutation angle, and extinction angle. In the following part, CCAT will be presented in two parts with the left and right parts of (1).

To analyze the energy demand for commutation, under steady operating conditions, the integration of the left side of (1) during commutation is:

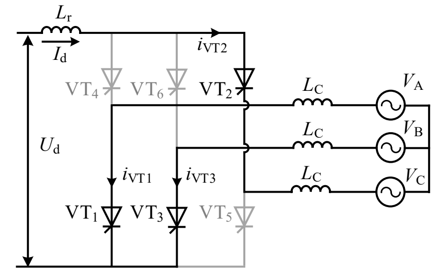

Fig. 1. The model of 6-pulse three-phase bridge.

$$\begin{aligned}&\int_{t_2}^{t_1}\left(L_C \frac{di_1(t)}{dt} - L_C \frac{di_3(t)}{dt}\right)dt \\ &= L_C\left\{\left[i_1(t_2)-i_1(t_1)\right]-\left[i_3(t_2)-i_3(t_1)\right]\right\} = -2L_c I_d\end{aligned} \tag{2}$$

The integration in (2) yields a constant value when the DC current $I_d$ is maintained. The integration of the AC bus voltage on the inverter side over time is referred to the commutation voltage-time area and is represented by the abbreviation $S_\mu$. Thus, the result derived from (2) serves as the critical commutation area that fulfills the DC system's requirements during steady operating conditions. Consequently, the demand of commutation area $S_{\mu,\text{demand}}$ is defined as:

$$S_{\mu,\text{demand}} = 2L_c I_d \tag{3}$$

The physical meaning of $S_{\mu,\text{demand}}$ is the external energy required by the valve inductor to establish the magnetic chain and commutate from $VT_1$ to $VT_3$.

To analyze the energy supply for commutation, under steady operating conditions, the integration of the right side of (1) during commutation is:

$$\int_{t_2}^{t_1} \sqrt{2}U_{si} \sin \omega t dt = \sqrt{2}U_{si}\left(\cos\gamma + \cos\alpha\right) \triangleq S_{\mu,\text{supply}} \tag{4}$$

The supply of commutation area, denoted as $S_{\mu,\text{supply}}$, represents the actual commutation area accumulated by $U_{si}$. From an energy perspective, $S_{\mu,\text{supply}}$ corresponds to the energy stored in the magnetic chain formed within the valve inductor.

If $S_{\mu,\text{supply}}$ is greater than or equal to $S_{\mu,\text{demand}}$, the requirement of commutation area is satisfied, enabling successful commutation of the DC system. Otherwise, if $S_{\mu,\text{supply}}$ is smaller than $S_{\mu,\text{demand}}$, the DC system would experience commutation failure.

In summary, CCAT establishes the relationship between commutation failure and the equilibrium of $S_{\mu,\text{demand}}$ and $S_{\mu,\text{supply}}$. The system's prerequisite for successful commutation is that the supply of commutation area satisfies the requirement.

### *B. Commutation Capability Index $S_{CCI}$*

To quantitatively evaluate DC system's commutation capability, this subsection proposes a commutation capability index considering the variant's fluctuations based on the modified CCAT.

The equations in (3) and (4) are derived based on the assumption that the $I_d$ and $U_{si}$ maintain constant during commutation process. To accurately evaluate the demand and supply of $S_\mu$, the fluctuations of $I_d$ and $U_{si}$ need to be taken into account [23]. Thus, the modified demand and supply of $S_\mu$ are as follows:

$$\begin{cases} S^*_{\mu,\mathrm{demand}} = 2L_c(I_d + \Delta I_d) \\ S^*_{\mu,\mathrm{supply}} = \sqrt{2}(U_{si} + \Delta U_{si})(\cos\gamma + \cos\alpha) \end{cases} \tag{5}$$

Where, $\Delta I_d$ and $\Delta U_{si}$ is the expression for the Taylor expansion of the $I_d$ and $U_{si}$ at the moment of fault occurrence $t_0$, neglecting the second order and higher residual terms.

$\Delta I_d$ and $\Delta U_{si}$ can be expressed as:

$$\begin{cases} \Delta I_d(\Delta t) = \dfrac{\mathrm{d}I_d(t_0)}{\mathrm{d}t}\Delta t + \dfrac{\mathrm{d}^2 I_d(t_0)}{\mathrm{d}t^2}\dfrac{\Delta t^2}{2} \\ \Delta U_{si}(\Delta t) = \dfrac{\mathrm{d}U_L(t_0)}{\mathrm{d}t}\Delta t + \dfrac{\mathrm{d}^2 U_L(t_0)}{\mathrm{d}t^2}\dfrac{\Delta t^2}{2} \end{cases} \tag{6}$$

Where, $\Delta t$ can be taken as 1.11ms, referring to the time corresponding to the lower limit of $\alpha$ (20°) with $f$=50Hz.

Besides, to ensure normal commutation, $\gamma$ needs to be larger than the limit extinction angle $\gamma_0$. In practical engineering, $\gamma_0$ is typically set to 7.2° [24]. In this case, the maximum of $S^*_{\mu,\mathrm{supply}}$ is given by:

$$S^*_{\mu,\mathrm{supply,max}} = \sqrt{2}(U_{si} + \Delta U_{si})(\cos\gamma_0 + \cos\alpha) \tag{7}$$

To avoid the occurrence of commutation failure, $S^*_{\mu,\mathrm{supply,max}}$ should be no less than $S^*_{\mu,\mathrm{demand}}$, i.e., satisfy (8):

$$\sqrt{2}(U_{si} + \Delta U_{si})(\cos\gamma_0 + \cos\alpha) - 2L_c(I_d + \Delta I_d) \geq 0 \tag{8}$$

The evaluation of DC system's commutation capability aims to determine its ability to mitigate commutation failure. Thus, by utilizing (8), the commutation capability index $S_{CCI}$ can be formulated based on the system's ability to deliver sufficient energy. $S_{CCI}$ is defined as follows:

$$S_{CCI} = \sqrt{2}(U_{si} + \Delta U_{si})(\cos\gamma_0 + \cos\alpha) - 2X_c(I_d + \Delta I_d) \tag{9}$$

The $S_{CCI}$ reflects the interrelationship and constraint among the three factors, $U_{si}$, $\alpha$, and $I_d$, which addresses the under-compensation issue caused by using single influencing factor as a control criterion.

Fig. 2 proves the effectiveness of the $S_{CCI}$ on indicating the occurrence and severity of commutation failure, which is supported by the consistent among $S_{CCI}$, extinction angle, and valve current. It is known that the extinction angle falling to zero indicates the occurrence of commutation failure, and the amplitude of valve current is related to the energy demand of

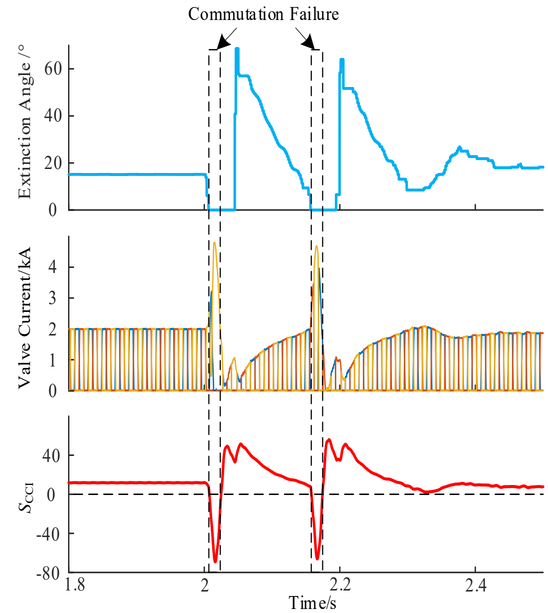

Fig. 2. System responses during subsequent commutation failure

commutation [19]. Therefore, from the consistent between $S_{CCI}$ and extinction angle, it is proved that $S_{CCI}$ can serve as an indicator to determine the occurrence of SCF: when $S_{CCI} \geq 0$, the DC system is able to commutate; when $S_{CCI} < 0$, commutation failure occurs. From the consistent between $S_{CCI}$ and valve current, it is proved that a smaller $S_{CCI}$ value indicates a larger shortage in the energy required for commutation within the system. This characteristic is also consistent with the description of system commutation margin in [20], and is more comprehensive and accurate than solely focusing on the γ angle.

The real-time calculation of $S_{CCI}$ must balance accuracy with computational feasibility. While smaller $\Delta t$ values theoretically improve derivative estimation in (6) and index precision, practical implementation is constrained by the sampling frequency ($f_s$) of control systems. The nominal $\Delta t$=1.11ms corresponds to $f_s$≈600Hz for single-rate sampling. However, the computation in (6) requires three times sampling per step to calculate the second-order terms, corresponding to $f_s$=1800 Hz. Modern HVDC controllers typically operate at $f_s$≈2kHz. Therefore, Δt is deliberately assigned a value of 1.11 ms, which sufficiently accounts for device constraints while ensuring adequate accuracy. Computational burden is minimal: a conservative estimate of (6) and (9) requires 25 FLOPs per cycle, and about 22.5 kFLOPS per second. For industrial hardware, this represents < 0.0003% of processing resources, confirming real-time feasibility.

## III. Improved CEC Strategy Based on Commutation Capability Index

CEC plays a crucial role in suppressing SCF as it facilitates the rapid switch between CC and CEA by compensating extinction angle. Nevertheless, the existing CEC methods, which solely rely on commutation voltage drop $\Delta U_{si}$ as a control criterion, encounter challenges of over-compensation or under-compensation in extinction angle [15], [16]. Moreover, these

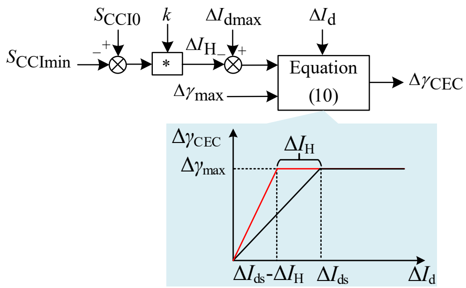


Fig. 3. Block diagram of $S_{CCI}$-based CEC slope dynamic calculation

methods show diminished effectiveness when dealing with asymmetrical faults.

In order to address the issues of over-compensation and under-compensation, this subsection introduces a dynamic calculation method for determining the CEC slope according to the evaluation of $S_{CCI}$ to commutation capability.

Based on the traditional CEC control, the proposed strategy changes the slope of CEC by adjusting $\Delta I_{ds}$ to obtain a more rational $\Delta\gamma_{CEC}$ for satisfying the requirement of commutation capability. The relationship between $\Delta I_d$ and $\Delta\gamma_{CEC}$ is given in (10).

$$\Delta\gamma_{\mathrm{CEC}} = \begin{cases} 0, & \Delta I_{\mathrm{d}} < 0 \\ k_{\mathrm{H}}\Delta I_{\mathrm{d}}, & 0 < \Delta I_{\mathrm{d}} \le \Delta I_{\mathrm{ds}} - \Delta I_{\mathrm{H}} \\ \Delta\gamma_{\max}, & \Delta I_{\mathrm{d}} > \Delta I_{\mathrm{ds}} - \Delta I_{\mathrm{H}} \end{cases} \qquad k_{\mathrm{H}} = \frac{\Delta\gamma_{\max}}{\Delta I_{\mathrm{ds}} - \Delta I_{\mathrm{H}}} \tag{10}$$

Where, $k_H$ is the modified slope of the CEC ramp function, and $\Delta I_H$ is the adjustment of $\Delta I_{ds}$.

The red curve in Fig. 3 represents the modified CEC ramp function curve. To ensure the economic operation of the system, this paper sets $\Delta\gamma_{max}$ as a constant value of 16° [15].

From the above analysis, it can be observed that increasing the slope of CEC enhances the value of $\Delta\gamma_{CEC}$, which facilitates the commutation recovery. Thus, the adjustment value $\Delta I_H$ is defined as:

$$\Delta I_{\mathrm{H}} = k_{\mathrm{S}}\Delta S_{\mathrm{req}} \tag{11}$$

Where $k_S$ is a proportional coefficient, and $\Delta S_{req}$ represents the difference between the actual value and the required value of $S_{CCI}$ during fault:

$$\Delta S_{\mathrm{req}} = S_{\mathrm{CCI0}} - S_{\mathrm{CCIreal}} \tag{12}$$

Where $S_{CCI0}$ represents the value of the $S_{CCI}$ under normal operation of the system, $S_{CCIreal}$ represents the calculated value of $S_{CCI}$ in real-time.

A larger $\Delta S_{req}$ indicates a more severe fault in the system increasing the risk of SCF. From (12), $\Delta S_{req}$ can be used to describe the energy deficit required for commutation during normal system operation. This energy deficit can be considered as the deficit in commutation voltage:

$$\Delta S_{\mathrm{req}} = U_{\mathrm{demand}}\Delta t \tag{13}$$

Where, $U_{demand}$ is the AC commutation voltage demand, $\Delta t$ is the fault duration.

To obtain the adjustments from DC control system, the AC commutation voltage demand should be converted to the DC voltage demand. From the expression for the average value of the DC voltage, the DC voltage demand can be derived as:

$$U_{\mathrm{dc,demand}} = \frac{2\sqrt{2}}{\pi}U_{\mathrm{demand}}\cos\gamma_{\mathrm{ref}} \tag{14}$$

Where $U_{dc,demand}$ represents the deficit in DC voltage, and the reference value for $\gamma$ is chosen to correspond to the deficit in DC voltage under normal operating conditions, typically set at 15°. The adjustment value of DC current reference $\Delta I_{dref}$ is calculated by VDCOL. In CIGRE benchmark HVDC model, $\Delta I_{dref}$ is calculated as follows:

$$\Delta I_{\mathrm{dref}} = m\frac{I_{\mathrm{dmax}} - I_{\mathrm{dmin}}}{U_{\mathrm{high}} - U_{\mathrm{low}}}\frac{U_{\mathrm{dc,demand}}}{U_{\mathrm{dB}}} \tag{15}$$

Where $m$ represents the proportion of the DC voltage deficit $U_{dc,demand}$ within the startup voltage range, $I_{dmax}$ is the maximum command value of VDCOL, $I_{dmin}$ is the minimum command value, $U_{high}$ is the high voltage threshold of VDCOL, $U_{low}$ is the low voltage threshold, and $U_v$ is the startup voltage, and $U_{dB}$ is the DC voltage reference.

From (11), (14), and (15), the proportional coefficient $k_H$ is defined as:

$$k_{\mathrm{S}} = \frac{2\sqrt{2}m\cos\gamma_{\mathrm{ref}}(I_{\mathrm{dmax}} - I_{\mathrm{dmin}})}{\pi U_{\mathrm{dB}}\Delta t(U_{\mathrm{high}} - U_{\mathrm{low}})} \tag{16}$$

Where, $\gamma_{ref}$ represents the reference value of the extinction angle, and $\Delta t$ represents the duration of the fault.

The specific calculation process of the proposed method is shown in Fig. 3. By utilizing the proposed dynamic calculation method, the slope of CEC can be adaptively adjusted based on $S_{CCI}$ to satisfy the demand of commutation. The control effect is further examined through simulations in Section IV.

## IV. Case Study

This section tests the effectiveness of the proposed control strategy under different fault severity levels within the CIGRE HVDC benchmark model [4]. Different fault severity levels were simulated by varying the grounding inductance.

The three control strategies used for simulation validation are as follows:

Control Strategy 1: CIGRE benchmark model control.

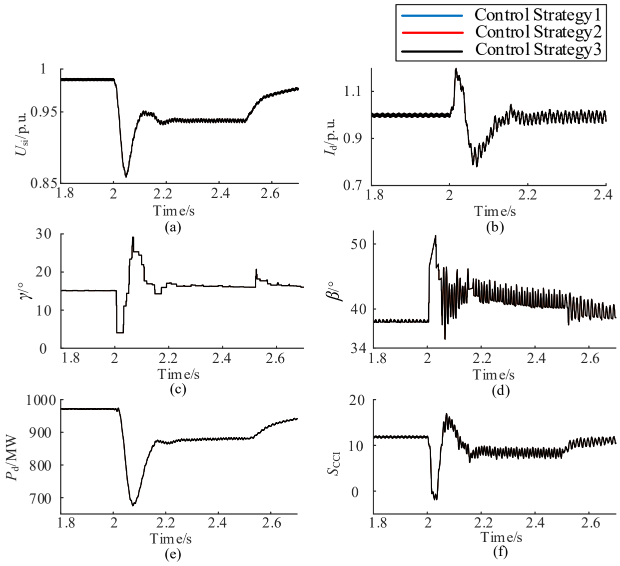


Fig. 4. System recovery characteristics under single-phase grounding failure ($L_f$=1H) (a) The inverter side bus voltage amplitude. (b) The DC current. (c) The extinction angle. (d) The advanced trigger angle of inverter. (e) The DC power. (f) The commutation capability index.

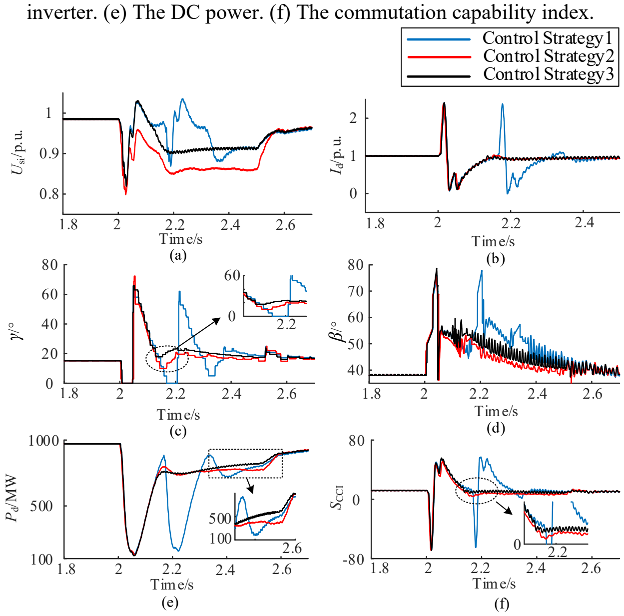


Fig. 5. System recovery characteristics under three-phase grounding fault ($L_f$=0.45H). (a) The inverter side bus voltage amplitude. (b) The DC current. (c) The extinction angle. (d) The advanced trigger angle of inverter. (e) The DC power. (f) The commutation capability index.

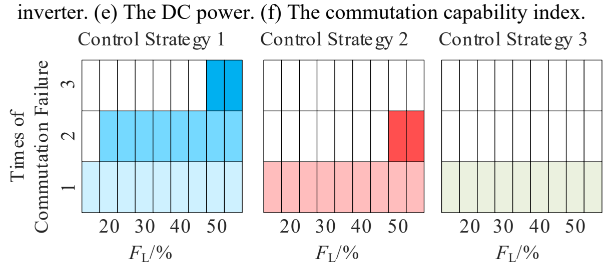


Fig. 6. Commutation failure times under three control strategies.

Control Strategy 2: Based on Control Strategy 1, CEC adopts the control method proposed in reference [16].

Control Strategy 3: Based on Control Strategy 1, CEC adopts the method proposed in this paper.

## *A. Case 1: Slight Asymmetric Fault*

In case 1, a single-phase grounding fault occurs at the inverter station's AC bus at 2 seconds. The grounding inductance is set to $L_f$ = 1H, and the fault duration is 0.05 seconds. The simulation results are depicted in Fig. 4. Case 1 simulates a slight AC fault that occurs in equivalent practical engineering. Fig. 4 indicates that, in case of this fault, the DC system has not experienced SCF, and Control Strategy 3 exhibits highly consistent system recovery characteristics with Control Strategy 1. This indicates that the control strategy proposed in this paper is only activated when there is a risk of SCF in the system and does not affect the fault recovery capability of the DC system. This case demonstrates the accuracy and reasonableness of the initiation criterion proposed in this paper for the dynamic CEC control strategy.

## *B. Case 2: Severe Asymmetric Fault*

In case 2, a three-phase grounding fault occurs at the inverter station's AC bus at 2 seconds. The grounding inductance is set to $L_f$ = 0.45H, and the fault duration is 0.05 seconds. The electrical quantity simulation response characteristics are depicted in Fig. 5. Case 2 simulates a severe symmetric AC fault occurring in equivalent practical engineering. Fig. 5 shows that Control Strategies 2 and 3 can improve the margin of $\gamma$ and enhance the system's recovery performance during the fault period. However, after fault clearance, the recovery performance of Control Strategy 2 deteriorates. Through comparative analysis, it is found that the improved CEC control strategy stops operating after $S_{CCI}$ is restored to positive, without affecting the subsequent recovery process of the system. In contrast, Control Strategy 2, which uses voltage magnitude drop as the startup criterion, cannot determine the actual commutation demand. As a result, it excessively compensates $\gamma$ after fault clearance, leading to a negative impact on the fault recovery process. During fault recovery, Strategy 2 exhibits a minimum voltage of 0.85 p.u., whereas the proposed Strategy 3 maintains 0.90 p.u., indicating superior recovery performance. The simulation results of this case validate the superiority of the $\Delta S_{req}$ based dynamic adjustment of the CEC slope function's slope method.

## *C. Different Severity Levels*

To further validate the inhibitory effect of the proposed control strategy on SCF, it is necessary to conduct simulation experiments with a variety of AC faults of different severity levels. The fault level, denoted as $F_L$, can be defined as follows [25]:

$$F_L = \frac{U_L^2}{L_f P_N} \times 100\% \tag{17}$$

Simulation experiments were conducted to verify the effects of different severity levels of single-phase and three-phase AC faults within an $F_L$ range of 5% to 50%. The number of commutation faults is shown in Fig. 6. From Fig. 6, it can be observed that for different fault levels and types of faults, Control Strategy 3 effectively suppresses the occurrence of SCF in the HVDC system.

In conclusion, the control strategy proposed in this paper demonstrates superior control performance compared to the other two strategies. This method not only enhances the margin of $\gamma$ during faults but also improves the system's fault recovery characteristics, thereby reducing the risk of SCF.

## V. Conclusion

This paper proposes an index, $S_{CCI}$, to evaluate the DC system's commutation capability. On the basis of $S_{CCI}$, an improved CEC strategy is proposed for SCF suppression. The conclusions of this paper can be summarized as follows.

1) Based on CCAT, the proposed index $S_{CCI}$ can accurately evaluate the system's commutation capability due to considering the fluctuations of the electrical variations.

2) The proposed dynamic CEC slope method, based on $S_{CCI}$, effectively suppresses SCF and enhances post-fault recovery performance.

3) Case studies confirm the strategy's robustness, demonstrating significant SCF suppression across fault severities (5%-50% $F_L$), improved $\gamma$ margin during faults, and superior recovery characteristics.

## References


[1] Z. Y. Liu, X. H. Qin, L. Zhao, and Q. B. Zhao, "Study on the ap-plication of UHVDC hierarchical connection mode to multi-infeed HVDC system," Proceedings of the Chinese Society of Electrical Engineering, vol. 33, no. 10, pp. 1–7, Apr. 2013.

[2] J. R. Shan, C. R. Liu, H. Li, and W. Wei, "Closed-loop Dynamic Phasor Simulation Model of LCC-HVDC Considering Phase-locked Loop and Commutation Failure," Proceedings of the Chinese Society of Electrical Engineering, vol. 41, no. 9, pp. 3046–3055, May. 2021.

[3] Y. Y. He, X. D. Zheng, N. L. Tai, J. X. Hou, J. Xu, and W. T. Huang, "A Review of Modeling Methods for LCC-HVDC Convert-er in AC/DC Hybrid Power Grid," Proceedings of the Chinese Society of Electrical Engineering, vol. 39, no. 11, pp. 3119–3129, Jun. 2019.

[4] C. R. Liu, A. Bose, P. F. Tian, "Modeling and analysis of HVDC converter by three-phase dynamic phasor," IEEE Transactions on Power Delivery, vol. 29, no.1, pp. 3-12, Feb. 2014.

[5] J. R. Shan, C. R. Liu, H. Luan, and W. Wei, "Closed-loop Dynamic Phasor Simulation Model of LCC-HVDC Considering Phase-locked Loop and Commutation Failure," Proceedings of the Chinese Society of Electrical Engineering, vol. 41, no. 9, pp.3046-3055, May. 2021.

[6] B. Rehman, C. R. Liu, H. Li, C. Fu, and W. Wei, "Analysis on Local and Concurrent Commutation Failure of Multi-infeed HVDC Considering Inter converter Interaction," Journal of Modern Power Systems and Clean Energy, vol. 10, no.4, Jul. 2022.

[7] M. J. Li, "Characteristic analysis and operational control of large-scale hybrid UHV AC/DC power grids," Power System Technology, vol. 40, no. 4, pp. 985–991, Apr. 2016.

[8] J. Z. Song, Y. L. Li, L. Zeng, and Y. K. Zhang, "Review on Com-mutation Failure of HVDC Transmission System," Automation of Electric Power Systems, vol. 44, no. 22, pp. 2–13, Nov. 2020.

[9] H. I. Son and H. M. Kim, "An algorithm for effective mitigation of commutation failure in high-voltage direct-current systems," IEEE Trans. Power Del., vol. 31, no. 4, pp. 1437-1446, Aug. 2016.

[10] F. Wang, T. Q. Liu, and X. Y. Li, "Decreasing the frequency of HVDC commutation failures caused by harmonics," IET Power Electronics, vol. 10, no. 2, pp. 215-221, Sept. 2016.

[11] S. Mirsaeidi and X. Z. Dong, "An Enhanced Strategy to Inhibit Commutation Failure in Line-Commutated Converters," IEEE Transactions on Industrial Electronics, vol. 67, no.1, Jan. 2020.

[12] L. R. Hong, X. P. Zhou, Y. F. Liu, H. T. Xia, H. H. Yin, Y. D. Chen, L. M. Zhou, and Q. M. Xu, "Analysis and Improvement of the Multiple Controller Interaction in LCC-HVDC for Mitigating Repetitive Commutation Failure," IEEE Transactions on Power De-livery, vol. 36, no. 4, pp. 1982–1991, Aug. 2021.

[13] L. Liu, S. Lin, J. Liu, P. Y. Sun, X. P. Li, and Z. Y. He, "Mechanism Analysis of Subsequent Commutation Failures Caused by Improper Interaction of Controllers," Power System Technology, vol. 43, no. 10, pp. 3562–3568, Oct. 2019.

[14] M. X. Han, and A. M. Gole, Modelling and Simulation of HVDC Transmission. London, United Kingdom, IET, 2021.

[15] H. T. Xia, X. P. Zhou, L. R. Hong, Y. F. Liu, A. Lou, X. Wang, and Q. Q. Meng, "An Adaptive Current Deviation Control Method for Suppressing Following Commutation Failures," Proceedings of the Chinese Society of Electrical Engineering, vol. 39, no. 15, pp. 4345–4355, Aug. 2019.

[16] Z. X. Dai, X. Y. Pan, and J. Y Wang, "Suppression Method for Continuous Commutation Failure Based on Dynamic Current Deviation Control," Proceedings of the CSU-EPSA, vol. 33, no. 3, pp. 49–58, May 2020.

[17] X. F. Song, W. W. Chen, B. H. Zhou, F. T. Li, Y. L. Xu, and J. Ren, "Influence of current error controller on commutation failures and system recovery," Electric Power Engineering Technology, vol. 41, no. 2, pp. 37–44, May. 2022.

[18] Y. L. Wang, X. H. Li, H. Li, S. Y. Li, and Y. X. Zheng, "A constant extinction angle acceleration control method for suppressing continuous commutation failure," Power System Protection and Control, vol. 52, no. 4, pp. 56-66, Feb. 16, 2024.

[19] C. Y. Guo, C. H. Li, Y. C. Liu, B. S. Jiang, C. Y. Zhao, and Q. Y. Zhou, "A DC Current Limitation Control Method Based on Virtu-al-resistance to Mitigate the Continuous Commutation Failure for Conventional HVDC," Proceedings of the Chinese Society of Electrical Engineering, vol. 36, no. 18, pp.4930-4937, Sept. 2016.

[20] "IEEE Guide for Planning DC Links Terminating at AC Locations Having Low Short-Circuit Capacities," in *IEEE Std 1204-1997*, 21 Jan. 1997.

[21] L. Liu, S. Lin, and Z. Y. He, "A Novel Method Based on Virtual Commutation Area Insufficient to Mitigate the Continuous Com-mutation Failure for HVDC," Proceedings of the Chinese Society of Electrical Engineering, vol. 38, no. 18, pp. 5361–5368, Sept. 2018.

[22] F. Cheng, L. Z. Yao, Z. B. Wang, C. X. Liu, Q. Q. Wang, J. P. Deng, and T. K. Lan, "A Commutation Failure Mitigation Strategy Based on Virtual Phase Lock Loop Voltage," Proceedings of the CSEE, vol. 40, no. 9, pp. 2756-2765, May. 2020.

[23] Z. X. Li, C. R. Liu, Y. Zuo, and Y. B. Shi, "Subsequent Commutation Failure Suppression Method Based on Optimized Current Error Controller Parameters" in SPIES, 2022, pp.1208-1212, Dec. 2022.

[24] B. H. Zhou, F. T. Li, and C. Y. Yin, "Risk Evaluation and Sup-pression Methods for Subsequent Commutation Failure of HVDC Transmission System," Automation of Electric Power Systems, vol. 45, no. 5, pp. 143–151, Mar. 2021.

[25] J. M. Wang, Q. Xu, P. Dai, G. Z. Wang, G. J. Shen, and H. H. Xin, "Suppression Method of Subsequent Commutation Failure Based on Reactive Power Feedback Control," Automation of Electric Power Systems, vol. 45, no. 12, pp. 101–108, Jun. 2021.

[26] X. P. Cong, X. D. Zheng, Y. Q. Cao, N. L. Tai, Y. C. Miu, and K. Li, "A Suppression Strategy for Subsequent Commutation Failures Considering Commutation Capability of Recovery Process," Journal of Shanghai Jiao Tong University, vol. 56, no. 3, pp. 333–341, Mar. 2022.